



Fat depot-specific differences of macrophage infiltration and cellular senescence in obese bovine adipose tissues

Tomoya YAMADA^{1)*}, Mituru KAMIYA¹⁾, Mikito HIGUCHI¹⁾ and Naoto NAKANISHI¹⁾

¹⁾Institute of Livestock and Grassland Science, National Agriculture and Food Research Organization, Nasushiobara-shi, Tochigi 329-2793, Japan

ABSTRACT. Obesity is associated with the chronic inflammation and senescence of adipose tissues. Macrophage is a key mediator of chronic inflammation that infiltrates obese adipose tissue and stimulates metabolic disorders. However, the fat depot-specific differences of macrophage infiltration and senescence, especially the influence on intramuscular adipose tissue, have remained unclear. We investigated the fat depot-specific differences of macrophage infiltration and senescence in obese bovine adipose tissue from three different anatomical sites (subcutaneous, intramuscular and visceral). Macrophage infiltrations and crown-like structures were observed in visceral adipose tissue, although there were few macrophages in subcutaneous and intramuscular adipose tissues. The positive reaction of senescence marker SA- β gal activity was observed in visceral adipose tissue. In contrast, the activity of SA- β gal in subcutaneous and intramuscular adipose tissues were low. The expression of p53 gene, the master regulator of cellular senescence, in visceral adipose tissue was higher than that of subcutaneous and intramuscular adipose tissue. At the cellular level, p53 gene expression was negatively correlated with the size of subcutaneous adipocytes. In contrast, p53 gene expressions were positively correlated with the size of intramuscular and visceral adipocytes. These results indicate that anatomical sites of obese adipose tissue affect macrophage infiltration and the senescent state in a fat depot-specific manner.

KEY WORDS: adipocyte, intramuscular adipose tissue, macrophage, senescence

J. Vet. Med. Sci.

80(10): 1495–1503, 2018

doi: 10.1292/jvms.18-0324

Received: 11 June 2018

Accepted: 2 August 2018

Published online in J-STAGE:
15 August 2018

Obesity is associated with the chronic inflammation of adipose tissue. Adipose tissue inflammation influences the risk of metabolic syndrome in a fat depot-specific manner. Excess visceral adipose tissue accumulation is closely related to the risk of metabolic disorders [10]. In contrast, subcutaneous adipose tissue has been shown to exhibit less inflammation than visceral adipose tissue, even in obese conditions [6, 11]. Macrophage is a key mediator of inflammation, which infiltrates into adipose tissue and stimulates metabolic disorders via increased expression of proinflammatory cytokines [1, 50]. Macrophage infiltration is more abundant in visceral adipose tissue than in subcutaneous adipose tissue of obese mice [2, 31]. These results indicate the crucial role of macrophage in the regulation of obesity-induced metabolic disorders through visceral adipose tissue inflammation.

Obesity is also strongly associated with the senescence of adipose tissue. Tumor suppressor p53 (p53) is a transcription factor that acts by inducing cellular senescence and promoting cell death [26]. The expression of p53 in adipose tissue was significantly higher in obese mice than in controls [53]. The upregulation of p53 in obese mouse adipose tissue increased macrophage infiltration and elevated the activity of senescence-associated β -galactosidase (SA- β gal), a marker of cellular senescence [28]. In contrast, the inhibition of p53 in obese mouse adipose tissue markedly decreased macrophage infiltration and suppressed the SA- β gal activity [28]. These results indicate the importance of p53 as a key regulator of obesity-induced adipose tissue inflammation and senescence. However, the fat depot-specific differences of p53 expression have remained unclear.

Hypoxia is also a potent inducer of adipose tissue inflammation. Hypoxia-inducible factor 1 α (HIF-1 α) is a transcription factor that regulates oxygen homeostasis and physiological responses to oxygen deprivation [3]. The adipocyte-specific overexpression of HIF-1 α in obese mice increases adipose tissue inflammation [14]. In addition, adipocyte-specific HIF-1 α knockout in obese mice reduces adipose tissue inflammation [23]. These results indicate that HIF-1 α plays a key role in adipose tissue inflammation. However, few studies have examined the relationship between HIF-1 α expression and adipose tissue depots.

Recently, ectopic fat deposition, especially intramuscular adipose tissue accumulation within the skeletal muscle, has

*Correspondence to: Yamada, T.: toyamada@affrc.go.jp

©2018 The Japanese Society of Veterinary Science



This is an open-access article distributed under the terms of the Creative Commons Attribution Non-Commercial No Derivatives (by-nc-nd) License. (CC-BY-NC-ND 4.0: <https://creativecommons.org/licenses/by-nc-nd/4.0/>)

Table 1. Characteristics of animals

	Age (month)	Body weight (kg)	Subcutaneous fat weight (kg)	Visceral fat weight (kg)	Intramuscular fat content (%)
Means \pm SE	30 \pm 0.3	714 \pm 18.5	55 \pm 3.3	51 \pm 2.4	34 \pm 2.1
Range	27–32	633–871	37–79	35–73	21–54

been recognized as a new risk factor of metabolic syndrome [5, 45]. However, the macrophage infiltration and senescence in intramuscular adipose tissue, in both humans and rodents, has not yet been investigated. In beef cattle, the amount of intramuscular adipose tissue is especially important for determining the quality grade of beef. In particular, Japanese black cattle (*Wagyu*) are characterized by the ability to accumulate high amounts of intramuscular adipose tissue [30]. Intramuscular fat percentages of longissimus muscles of fattening *Wagyu* cattle are typically higher than 30% [30], which is about ten times higher than the established animal model of intramuscular fat accumulation in Otsuka Long-Evans Tokushima fatty (OLETF) rat [49, 52]. Therefore, for elucidating the mechanism of intramuscular adipocyte metabolism, *Wagyu* is thought to be the optimal animal model rather than rodents.

In the present study, we investigated fat depot-specific differences of macrophage infiltration and senescence in obese *Wagyu* cattle from three different anatomical sites (subcutaneous, intramuscular, and visceral).

MATERIALS AND METHODS

Animals

Fattening *Wagyu* steers (n=15) were used in this study. The characteristics of animals are shown in Table 1. Subcutaneous adipose tissue and the intramuscular adipose tissue within the longissimus muscle were collected between the third and fourth lumbar vertebrae at slaughter. Visceral adipose tissue was also sampled from the area surrounding the colon. Adipose tissue samples for determining mRNA expression were collected immediately after slaughter in RNAlater reagent (Ambion, Foster City, CA, U.S.A.) and stored at -80°C for later RNA extraction. Thin slices of adipose tissue samples were also collected immediately after slaughter to determine the immunohistochemistry, adipocyte size, and senescence-associated β -galactosidase (SA- β gal) staining, as described below. After slaughter, the carcass was physically separated into muscle, bone, and fat to measure the subcutaneous and visceral fat tissue weight. The intramuscular fat content of the longissimus muscle was obtained via Soxhlet extraction method. All animals received humane care as outlined in the Guide for the Care and Use of Experimental Animals (Institute of Livestock and Grassland Science).

RNA isolation and real-time PCR

mRNA expression was analyzed by real-time PCR as described previously [54–56]. In brief, total RNA was extracted from adipose tissue using a RiboPure Kit (Ambion) in accordance with the manufacturer's instructions. First-strand cDNA was reverse-transcribed from 0.5 μg of total RNA using the ReverTra Ace qPCR RT Kit (Toyobo Co., Osaka, Japan) in accordance with the manufacturer's protocol. Real-time PCR was performed with a MiniOpticon system (Bio-Rad, Munich, Germany) using THUNDERBIRD SYBR qPCR Mix (Toyobo) in accordance with the manufacturer's instructions. The primer sequences were as follows: CD68, 5'- CAG AAG GCA GAG GGT ACA GG-3' (forward) and 5'- ACA CAG CCA ACC TCA TGA CA-3' (reverse); CD163, 5'- CTG TAA TCT GCT CAG GAA ATC G-3' (forward) and 5'- GCA AGG AAC ACC ATT CTC TTC-3' (reverse); TNF α , 5'- CCC ATC TAC CAG GGA GGA GT-3' (forward) and 5'- GGC GAT GAT CCC AAA GTA GA-3' (reverse); VEGF, 5'- GAA CTT TCT GCT CTC TTG GG-3' (forward) and 5'- CTG GCT TTG GTG AGG TTT GA-3' (reverse); mmp9, 5'- CCA TTA GCA CGC ACG ACA TC-3' (forward) and 5'- TTC ACC TCA TTC TGG GAA CTC AC-3' (reverse); p53, 5'- CTG AGT GCA CCA CCA TCC ACT A-3' (forward) and 5'- TGT TCC GTC CCA GCA GGT TA-3' (reverse); HIF-1 α , 5'- GCA ACC AGA TGA TCG TGC AA-3' (forward) and 5'- AAT CAT AAC TGG TCA GCT GTG GTA G-3' (reverse); ribosomal protein large P0 (RPLP0), 5'-CAA CCC TGA AGT GCT TGA CAT-3' (forward) and 5'-AGG CAG ATG GAT CAG CCA-3' (reverse). Reaction conditions were designed as follows: initial denaturation at 95°C for 60 sec, followed by 40 cycles at 95°C for 15 sec, 55°C for 15 sec, and 70°C for 30 sec. Expression levels of mRNA were normalized to RPLP0 as an internal control.

SA- β gal staining

SA- β gal activity was examined using the Senescence Detection Kit (BioVision Co., Milpitas, CA, U.S.A.). In brief, adipose tissue samples were incubated within X-gal staining solution overnight at 37°C in the dark, followed by washing two times with ice-cold PBS to stop the enzymatic reaction. Stained adipose tissues were photographed using a digital camera (DMC-TZ85, Panasonic, Tokyo, Japan). SA- β gal-positive adipocytes within adipose tissues form a blue precipitate area [28].

Immunohistochemistry

For immunohistochemistry, frozen sections (10–12 μm) were cut from adipose tissues with a cryostat (CM1850, Leica, Wetzlar, Germany). Macrophages were identified using the VECTASTAIN Elite ABC Kit (Vector, Burlingame, CA, U.S.A.) in accordance with the manufacturer's instructions. In brief, sections were incubated overnight (4°C) with primary monoclonal anti-CD68 (1:300,

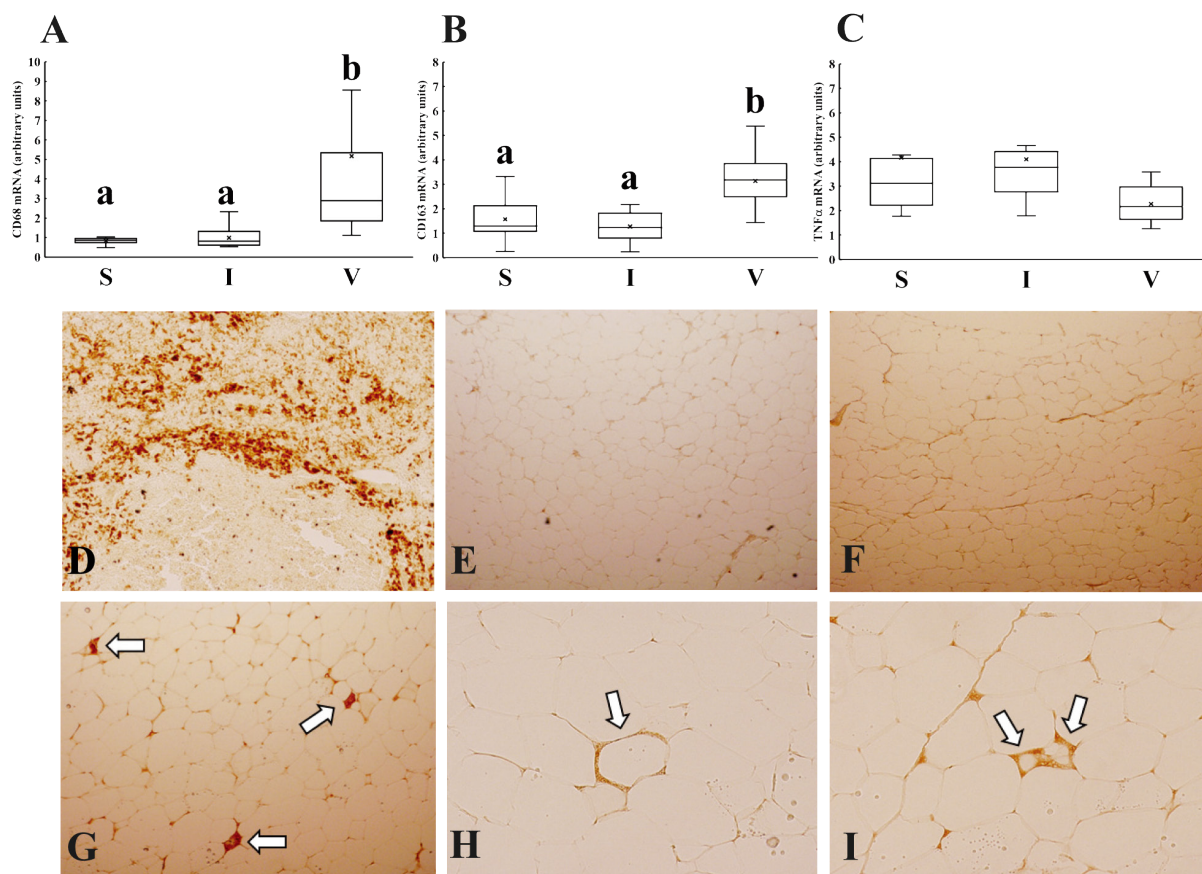


Fig. 1. Fat depot-specific differences of macrophage infiltration in obese bovine adipose tissues. Expression of the macrophage marker gene ((A) CD68 and (B) CD163), and (C) TNF α gene in subcutaneous (S), intramuscular (I), and visceral (V) adipose tissue (n=15). The middle line in the box-plot represents the median, and the vertical bars indicate the range of data. a, b: Values with different superscripts were significantly different ($P<0.05$). Representative light-microscopic images of (D) bovine spleen (positive control), (E) subcutaneous adipose tissue, (F) intramuscular adipose tissue, and (G, H, I) visceral adipose tissue. (G) CD68 immunoreactive macrophages and (H, I) crown-like structures (CLS) within visceral adipose tissue are indicated by white arrowheads (magnification: (D, E, F, G) $\times 40$, (H, I) $\times 100$).

clone EBM11, Dako, Glostrup, Denmark), and secondary antibodies were labeled with peroxidase (1:1,000, PK-6102, Vector) for 2 hr at room temperature. The immunoreaction was visualized using the ImmPACT DAB Substrate Kit (Vector) in accordance with the manufacturer's protocol. Stained sections were photographed using an IX71 microscope (Olympus, Tokyo, Japan) fitted with a DP70 digital camera (Olympus).

Adipocyte size

Adipocyte size was measured as described previously [39]. In brief, adipose tissue samples were fixed with 2% osmium tetroxide at room temperature. Then, fixed adipose tissue samples were incubated within 8 M of urea solution. Stained adipocytes were photographed using a microscope system (Olympus) as described above. The adipocyte diameter was measured using WinROOF software (Mitani Corp., Fukui, Japan). More than 300 adipocytes for each sample were measured.

Statistical analysis

Results are presented as means \pm S.D. Statistical significance was determined by analysis of variance (ANOVA), followed by Tukey's *post hoc* test. The linear regression method was used to analyze correlations. Values of $P<0.05$ were considered significant, and $0.05\leq P<0.1$ was considered a trend toward significance.

RESULTS

Fat depot-specific differences of macrophage infiltrations

Fat depot-specific differences in macrophage infiltration were measured in the three types of adipose tissues (subcutaneous, intramuscular, and visceral). CD68 and CD163 gene expressions were quantified as a marker of macrophage. Visceral adipose tissue expressed significantly higher CD68 ($P<0.05$, Fig. 1A) and CD163 ($P<0.05$, Fig. 1B) mRNA than did subcutaneous and intramuscular adipose tissues. There was no significant difference in the expression of TNF α mRNA among adipose tissue depots

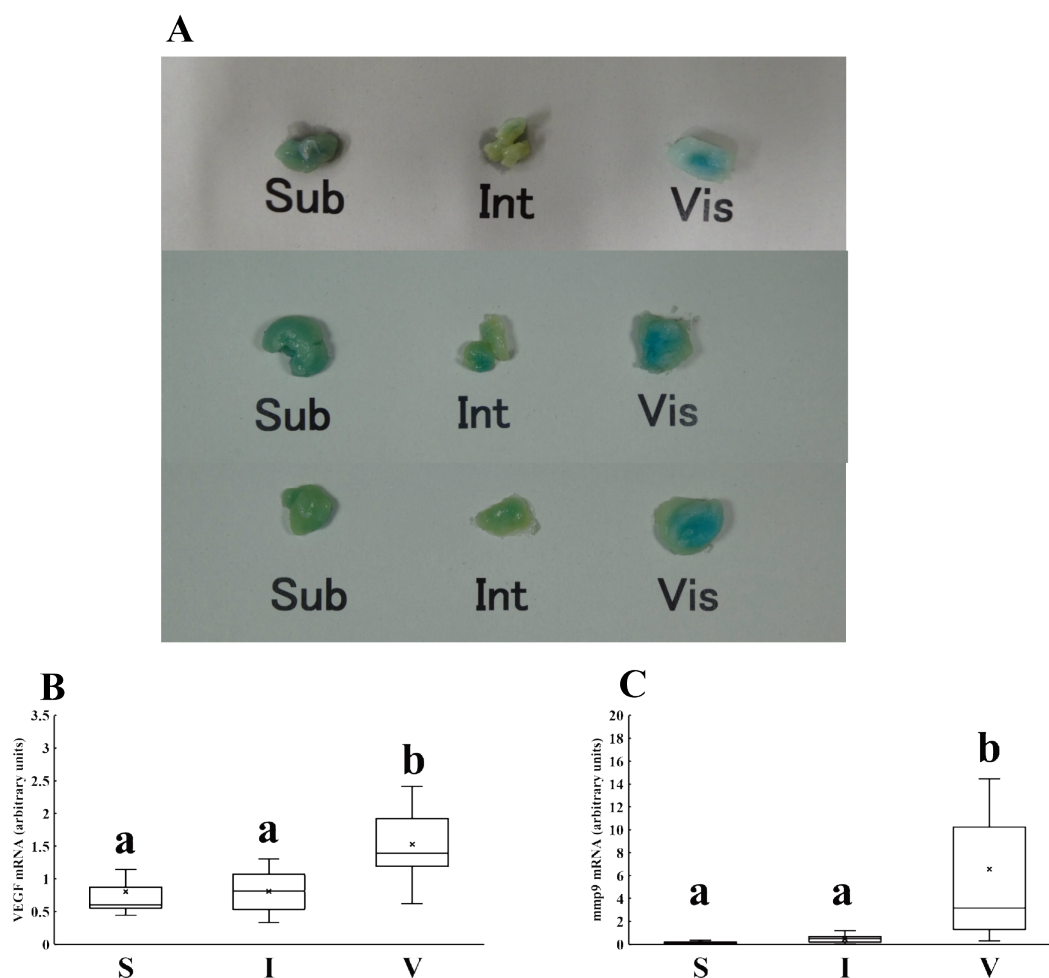


Fig. 2. Fat depot-specific differences of adipocyte senescence in obese bovine adipose tissues. (A) SA-βgal staining of subcutaneous (Sub), intramuscular (Int), and visceral (Vis) adipose tissue. SA-βgal activity (blue color) was observed in visceral adipose tissue. In contrast, the activity of SA-βgal in subcutaneous and intramuscular adipose tissues were low. Expression of the senescence-associated secretory phenotype (SASP) marker gene ((B) VEGF, and (C) mmp9) gene in subcutaneous (S), intramuscular (I), and visceral (V) adipose tissue. The middle line in the box-plot represents the median, and the vertical bars indicate the range of data. a, b: Values with different superscripts were significantly different ($P<0.05$).

(Fig. 1C). Then, we observed the macrophage infiltrations among subcutaneous, intramuscular, and visceral adipose tissues. There are few macrophages in subcutaneous (Fig. 1E) and intramuscular (Fig. 1F) adipose tissues. Macrophage infiltration was observed mainly in visceral adipose tissue (Fig. 1G). Crown-like structures (CLS), which consist of macrophages surrounding dead adipocytes [2, 7, 31], were also found only in visceral adipose tissue (Fig. 1H, 1I).

Fat depot-specific differences of adipose tissue senescence

Figure 2 shows fat depot-specific differences of adipose tissue senescence. The positive reaction of senescence marker SA-βgal activity (blue color) was observed in visceral adipose tissue (Fig. 2A). In contrast, the activity of SA-βgal in subcutaneous and intramuscular adipose tissues were low (Fig. 2A). Visceral adipose tissue also expressed significantly higher senescence-associated secretory phenotype (SASP) marker genes VEGF ($P<0.05$, Fig. 2B), and mmp9 ($P<0.05$, Fig. 2C) than did subcutaneous and intramuscular adipose tissues.

Figure 3 shows osmium tetroxide-fixed adipocytes from (S) subcutaneous, (I) intramuscular, and (V) visceral adipose tissues. Compared to visceral adipocytes, the subcutaneous and intramuscular adipocyte size distribution shifted toward smaller diameters (Fig. 3A). The mean adipocyte size increased significantly ($P<0.05$, Fig. 3B) in the following order: intramuscular ($133.0 \pm 9.2 \mu\text{m}$), subcutaneous ($144.6 \pm 9.1 \mu\text{m}$), and visceral ($183.7 \pm 12.8 \mu\text{m}$) adipocytes (Fig. 3C–E).

Figure 4 shows the p53 and HIF-1α gene expressions among three types of adipose tissues. Visceral adipose tissue expressed higher p53 mRNA than did subcutaneous and intramuscular adipose tissues (Fig. 4A). Morphological analysis of adipocytes showed that the p53 mRNA expression level was negatively correlated with the subcutaneous adipocyte size ($r=-0.69$, $P<0.01$, Fig. 4B). However, the p53 mRNA expression level was positively correlated with the intramuscular ($r=0.81$, $P<0.01$, Fig. 4C)

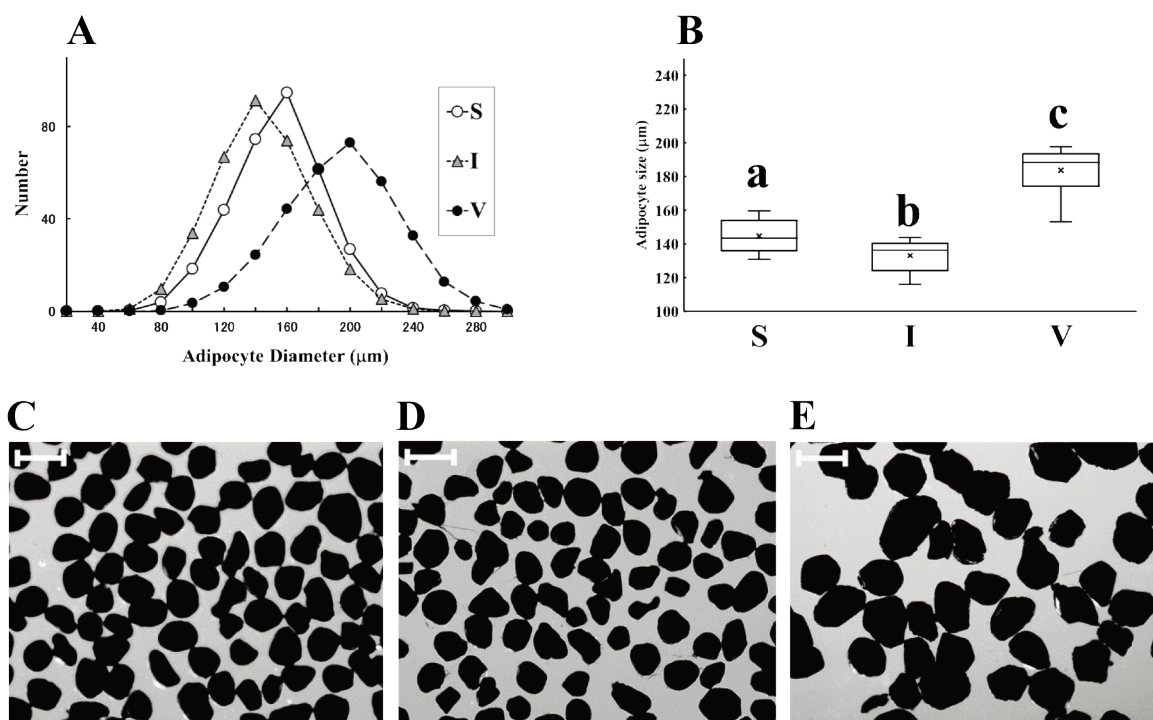


Fig. 3. Fat depot-specific differences of adipocyte cellularity in obese bovine adipose tissues. (A) Distributions of sizes of adipocyte diameter in subcutaneous (S), intramuscular (I), and visceral (V) adipose tissues (n=15). (B) Mean adipocyte diameter of subcutaneous (S), intramuscular (I), and visceral (V) adipose tissues. The middle line in the box-plot represents the median, and the vertical bars indicate the range of data. a, b, c: Values with different superscripts were significantly different ($P < 0.05$). Osmium tetroxide-fixed adipocytes from (C) subcutaneous, (D) intramuscular, and (E) visceral adipose tissues (magnification: $\times 40$). White scale bar indicates $300 \mu\text{m}$.

and visceral ($r=0.52$, $P < 0.01$, Fig. 4D) adipocyte sizes. In contrast, there was no significant difference in the expression of HIF-1 α mRNA among adipose tissue depots (Fig. 4E). HIF-1 α mRNA expression level was positively correlated with the subcutaneous adipocyte size ($r=0.51$, $P < 0.05$, Fig. 4F), and negatively correlated with intramuscular ($r=-0.51$, $P < 0.05$, Fig. 4G) and visceral ($r=-0.46$, $P=0.08$, Fig. 4H) adipocyte size.

DISCUSSION

In the present study, we showed that the macrophage infiltration into visceral adipose tissue was higher than that of subcutaneous and intramuscular adipose tissues. We also showed that there was no significant difference in the expression of TNF α gene among adipose tissue depots as previously reported in rat adipose tissues [32]. As for the macrophage infiltration into adipose tissues, previous reports also showed that macrophage infiltration was significantly higher in visceral adipose tissue than in subcutaneous adipose tissue in obese mice [2, 31] and humans [15, 25]. These results indicate that visceral adipose tissue is the most active adipose tissue depot as related to macrophage infiltration both in obese monogastric animals and obese ruminants. Our data for higher macrophage infiltration and CLS formation also suggest increasing adipocyte death within visceral adipose tissue. Alkhourri *et al.* reported that macrophage infiltration and adipocyte death were increased in the adipose tissue of obese mice [1]. Cinti *et al.* showed that the frequency of adipocyte death is positively correlated with increased adipocyte size in obese mice and humans [7]. We also showed that visceral adipocyte size was significantly larger than subcutaneous and intramuscular depots. Hypertrophic adipocytes ensured an insufficient oxygen supply and were affected by hypoxic stress [16, 17]. In addition, visceral adipose tissue is exposed to more stressors, such as oxidative stress and reactive oxygen species (ROS), than are subcutaneous locations [12, 24, 43]. These stressors stimulate adipocyte death via the accumulation of DNA damage [46]. Our previous study also showed that oxidative stress was strongly associated with visceral adiposity rather than subcutaneous adiposity in obese cattle [55]. These results suggest that increasing macrophage infiltration into visceral adipose tissue is affected by larger adipocyte size and more stressors than in subcutaneous and intramuscular adipose tissues.

We found that, by increased activity of SA- β gal, visceral adipose tissue exhibited an accelerated senescent phenotype as compared to subcutaneous and intramuscular tissues. To our knowledge, this study is the first to investigate fat depot-specific differences of SA- β gal activity, especially the senescent phenotype of ectopic (intramuscular) adipose tissue. Cellular senescence is categorized into two distinct types. "Replicative senescence" is associated with the cellular aging process affected by telomere shortening [35, 41]. In contrast, "premature senescence" is induced by stressors such as oxidative stress and ROS without

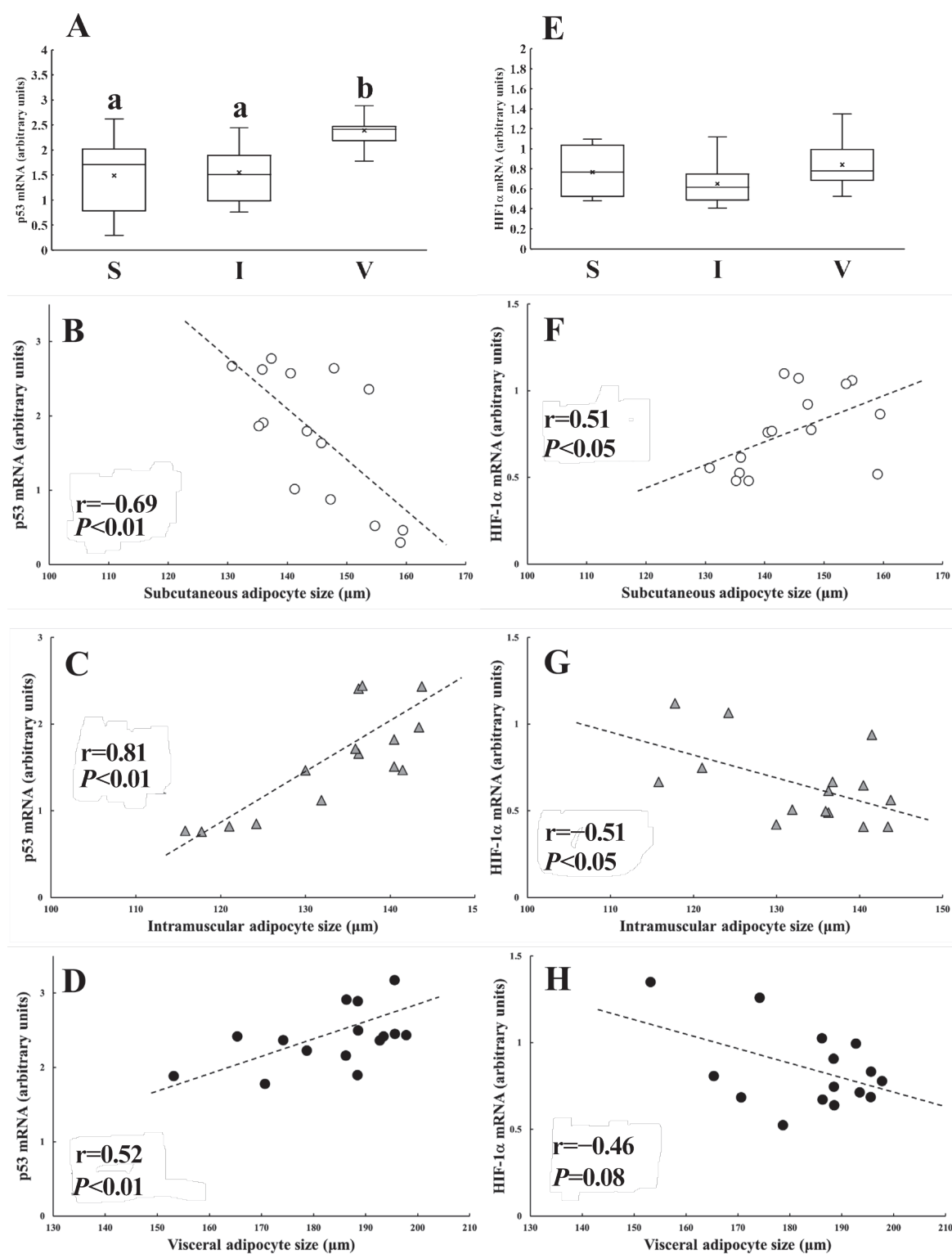


Fig. 4. Fat depot-specific differences of p53 and HIF-1 α mRNA expression in obese bovine adipose tissues. Expression of (A) p53 and (E) HIF-1 α genes in subcutaneous (S), intramuscular (I), and visceral (V) adipose tissues (n=15). The middle line in the box-plot represents the median, and the vertical bars indicate the range of data. a, b: Values with different superscripts were significantly different ($P < 0.05$). Relationship between p53 gene expression and (B) subcutaneous, (C) intramuscular, and (D) visceral adipocyte size. Relationship between HIF-1 α gene expression and (F) subcutaneous, (G) intramuscular, and (H) visceral adipocyte size. (○) subcutaneous adipocyte; (▲) intramuscular adipocyte; (●) visceral adipocyte.

telomere-independent mechanisms [51, 57]. Our previous study indicated that telomere length was not associated with adipocyte hypertrophy from three anatomical sites (subcutaneous, visceral and intramuscular) in obese cattle [56]. These results suggest that obese visceral adipose tissue is in a state of premature senescence. Premature senescence leads to a senescence-associated secretory phenotype (SASP) characterized by the increased production of cytokines and matrix metalloproteinase (mmp) [40, 42, 50]. In the present study, we showed that visceral adipose tissue expressed significantly higher SASP marker genes than did subcutaneous and intramuscular adipose tissues. Our previous study also indicated that obese bovine visceral adipocytes expressed higher levels of adipokine genes than did subcutaneous and intramuscular adipocytes [54]. These results also suggest that obese visceral adipose tissue is in a state of SASP.

We showed that visceral adipose tissue expressed highest levels of p53 among the three adipose tissue depots. The p53 signaling pathway is involved in the regulation of cellular senescence [26], and the upregulation of p53 in the adipose tissue of obese mice stimulates senescence-associated inflammation [28]. Shimizu *et al.* also showed that obese conditions cause ROS-induced upregulation of p53 in adipose tissue [47]. In addition, Schafer *et al.* showed that excessive nutrient intake upregulated the activity of SA- β gal, with increased expression of p53 in the adipose tissue of obese mice [42]. These results indicate that fat depot-specific differences of adipose tissue premature senescence and inflammation are regulated by p53. In contrast, no significant differences in the HIF-1 α expression level were observed among adipose tissue depots. Poulain-Godefroy *et al.* also reported that there was no difference in the HIF-1 α expression levels of subcutaneous and visceral adipose tissues in humans [36]. These results suggest that the HIF-1 α expression level in adipose tissue might not be affected by anatomical locations.

At the cellular level, the present results showed that the adipocyte sizes of subcutaneous and intermuscular/visceral depots were oppositely affected by p53 and HIF-1 α expression levels. In subcutaneous depots, hypertrophic adipocyte had lower p53 and higher HIF-1 α gene expression. In contrast to subcutaneous adipocytes, hypertrophic adipocytes in intermuscular and visceral depots had higher p53 and lower HIF-1 α gene expression. Ravi *et al.* reported that p53 inhibited the expression of HIF-1 α [37]. Mizuno *et al.* also showed that p53 knockout mice displayed higher HIF-1 α expression levels than did wild-type mice [29]. These results suggest that the HIF-1 α levels in adipocytes are negatively affected by p53 expression. Sermeus *et al.* indicated that under mild hypoxic conditions, a high intracellular level of HIF-1 α is maintained with a low p53 level, which stimulates the expression of target genes involved in cellular survival and protects against cell death [44]. In contrast, anoxic conditions induce high p53 and low HIF-1 α levels, which leads to cell death [44]. These results suggest that, at the cellular level, hypertrophic adipocytes might be exposed to more severe hypoxic conditions in visceral and intramuscular depots than in subcutaneous locations.

Daviau *et al.* indicated that p53 expression was significantly up-regulated in Preadipocyte factor-1 (pref-1) knockdown WI-38 cells [8]. Pref-1 is a transmembrane protein acts as a molecular gatekeeper of adipogenesis [48]. Our previous reports showed that pref-1 gene expression level was fat-depot specific, and pref-1 expression level was positively correlated with the subcutaneous adipocyte size, and negatively correlated with the intramuscular and visceral adipocyte size [56]. These results suggest that p53 expression might be regulated negatively by the pref-1 pathway. Further studies are needed to clarify the effects of pref-1 on the p53 expression during adipogenesis.

In fattening *Wagyu* cattle, obesity-associated adipose tissue disorders, called “fat necrosis” and “muscle inflammation”, occasionally develop during fattening periods [18, 34]. The histological analysis of bovine fat necrosis shows an increasing fibrous area within visceral adipose tissue [20]. Obese conditions accelerate the fibrosis of adipose tissue as a cause of severe inflammation both in humans [9, 38] and rodents [21, 22]. These results suggest that “fat necrosis” of bovine visceral adipose tissue might be affected by the severe inflammatory condition induced by obesity. “Muscle inflammation” is generally observed at the musculus trapezius and longissimus dorsi of fattening *Wagyu* cattle; these musculatures contain the largest amount of intramuscular adipose tissue among bovine muscles [18, 19]. The histological analysis of bovine “muscle inflammation” is characterized by muscular steatosis [4, 33]. A murine model of nonalcoholic fatty liver disease studies indicated that the expression of p53 was increased in hepatic steatosis [13, 53]. In addition, Liu *et al.* reported that subcutaneous adipose tissue was more resistant than visceral adipose tissue to cell death caused by oxidative stress [27]. These results also suggest that not only visceral adipocytes, but also intramuscular adipocytes might be potentially more sensitive than subcutaneous adipocytes for stress conditions induced by obesity.

In conclusion, we show that the macrophage infiltration into visceral adipose tissue is higher than that of subcutaneous and intramuscular adipose tissues. The present results also show that the fat depot-specific differences of adipose tissue premature senescence are affected by p53 expression. These results indicate that anatomical sites of obese adipose tissue affect macrophage infiltration and the senescent state in a fat depot-specific manner.

ACKNOWLEDGMENT. This work was supported by a Grant-in-Aid for Scientific Research (15K07699 and 18K05958) from the Japan Society for the Promotion of Science.

REFERENCES

1. Alkhoury, N., Gornicka, A., Berk, M. P., Thapaliya, S., Dixon, L. J., Kashyap, S., Schauer, P. R. and Feldstein, A. E. 2010. Adipocyte apoptosis, a link between obesity, insulin resistance, and hepatic steatosis. *J. Biol. Chem.* **285**: 3428–3438. [Medline] [CrossRef]
2. Altintas, M. M., Azad, A., Nayer, B., Contreras, G., Zaias, J., Faul, C., Reiser, J. and Nayer, A. 2011. Mast cells, macrophages, and crown-like structures distinguish subcutaneous from visceral fat in mice. *J. Lipid Res.* **52**: 480–488. [Medline] [CrossRef]
3. Ban, J. J., Ruthenborg, R. J., Cho, K. W. and Kim, J. W. 2014. Regulation of obesity and insulin resistance by hypoxia-inducible factors. *Hypoxia (Auckl.)* **2**: 171–183. [Medline]

4. Biasibetti, E., Amedeo, S., Brugiapaglia, A., Destefanis, G., Di Stasio, L., Valenza, F. and Capucchio, M. T. 2012. Lipomatous muscular ‘dystrophy’ of Piedmontese cattle. *Animal* **6**: 1839–1847. [[Medline](#)] [[CrossRef](#)]
5. Britton, K. A. and Fox, C. S. 2011. Ectopic fat depots and cardiovascular disease. *Circulation* **124**: e837–e841. [[Medline](#)] [[CrossRef](#)]
6. Bruun, J. M., Lihn, A. S., Madan, A. K., Pedersen, S. B., Schiøtt, K. M., Fain, J. N. and Richelsen, B. 2004. Higher production of IL-8 in visceral vs. subcutaneous adipose tissue. Implication of nonadipose cells in adipose tissue. *Am. J. Physiol. Endocrinol. Metab.* **286**: E8–E13. [[Medline](#)] [[CrossRef](#)]
7. Cinti, S., Mitchell, G., Barbatelli, G., Murano, I., Ceresi, E., Faloia, E., Wang, S., Fortier, M., Greenberg, A. S. and Obin, M. S. 2005. Adipocyte death defines macrophage localization and function in adipose tissue of obese mice and humans. *J. Lipid Res.* **46**: 2347–2355. [[Medline](#)] [[CrossRef](#)]
8. Daviau, A., Couture, J. P. and Blouin, R. 2011. Loss of DLK expression in WI-38 human diploid fibroblasts induces a senescent-like proliferation arrest. *Biochem. Biophys. Res. Commun.* **413**: 282–287. [[Medline](#)] [[CrossRef](#)]
9. Divoux, A., Tordjman, J., Lacasa, D., Veyrie, N., Hugol, D., Aissat, A., Basdevant, A., Guerre-Millo, M., Poitou, C., Zucker, J. D., Bedossa, P. and Clément, K. 2010. Fibrosis in human adipose tissue: composition, distribution, and link with lipid metabolism and fat mass loss. *Diabetes* **59**: 2817–2825. [[Medline](#)] [[CrossRef](#)]
10. Fox, C. S., Massaro, J. M., Hoffmann, U., Pou, K. M., Maurovich-Horvat, P., Liu, C. Y., Vasan, R. S., Murabito, J. M., Meigs, J. B., Cupples, L. A., D’Agostino, R. B. Sr. and O’Donnell, C. J. 2007. Abdominal visceral and subcutaneous adipose tissue compartments: association with metabolic risk factors in the Framingham Heart Study. *Circulation* **116**: 39–48. [[Medline](#)] [[CrossRef](#)]
11. Fried, S. K., Bunkin, D. A. and Greenberg, A. S. 1998. Omental and subcutaneous adipose tissues of obese subjects release interleukin-6: depot difference and regulation by glucocorticoid. *J. Clin. Endocrinol. Metab.* **83**: 847–850. [[Medline](#)]
12. Fujita, K., Nishizawa, H., Funahashi, T., Shimomura, I. and Shimabukuro, M. 2006. Systemic oxidative stress is associated with visceral fat accumulation and the metabolic syndrome. *Circ. J.* **70**: 1437–1442. [[Medline](#)] [[CrossRef](#)]
13. Ganz, M., Bukong, T. N., Csak, T., Saha, B., Park, J. K., Ambade, A., Kodys, K. and Szabo, G. 2015. Progression of non-alcoholic steatosis to steatohepatitis and fibrosis parallels cumulative accumulation of danger signals that promote inflammation and liver tumors in a high fat-cholesterol-sugar diet model in mice. *J. Transl. Med.* **13**: 193. [[Medline](#)] [[CrossRef](#)]
14. Halberg, N., Khan, T., Trujillo, M. E., Wernstedt-Asterholm, I., Attie, A. D., Sherwani, S., Wang, Z. V., Landskroner-Eiger, S., Dineen, S., Magalang, U. J., Brekken, R. A. and Scherer, P. E. 2009. Hypoxia-inducible factor 1 α induces fibrosis and insulin resistance in white adipose tissue. *Mol. Cell. Biol.* **29**: 4467–4483. [[Medline](#)] [[CrossRef](#)]
15. Harman-Boehm, I., Blüher, M., Redel, H., Sion-Vardy, N., Ovadia, S., Avinoach, E., Shai, I., Klötting, N., Stumvoll, M., Bashan, N. and Rudich, A. 2007. Macrophage infiltration into omental versus subcutaneous fat across different populations: effect of regional adiposity and the comorbidities of obesity. *J. Clin. Endocrinol. Metab.* **92**: 2240–2247. [[Medline](#)] [[CrossRef](#)]
16. Helmlinger, G., Yuan, F., Dellian, M. and Jain, R. K. 1997. Interstitial pH and pO₂ gradients in solid tumors in vivo: high-resolution measurements reveal a lack of correlation. *Nat. Med.* **3**: 177–182. [[Medline](#)] [[CrossRef](#)]
17. Hosogai, N., Fukuhara, A., Oshima, K., Miyata, Y., Tanaka, S., Segawa, K., Furukawa, S., Tochino, Y., Komuro, R., Matsuda, M. and Shimomura, I. 2007. Adipose tissue hypoxia in obesity and its impact on adipocytokine dysregulation. *Diabetes* **56**: 901–911. [[Medline](#)] [[CrossRef](#)]
18. Ishida, T., Noda, K., Jomane, F. N. and Tokunaga, T. 2017. Polymorphisms of RDH16 and VEGFR1 influence M. trapezius steatosis in Japanese Black carcass. *Anim. Sci. J.* **88**: 1037–1041. [[Medline](#)] [[CrossRef](#)]
19. Ishizuka, Y., Nishioka, T., Ohtani, S. and Irie, M. 2008. Factors affecting the incidence rate of beef carcass defect shikori. *Nihon Chikusan Gakkaiho* **79**: 497–506. [[CrossRef](#)]
20. Ito, T., Miura, S., Ohshima, K. and Numakunai, S. 1968. Pathological studies on fat necrosis (lipomatosis) in cattle. *Nippon Juigaku Zasshi* **30**: 141–150. [[Medline](#)] [[CrossRef](#)]
21. Kawanishi, N., Niihara, H., Mizokami, T., Yano, H. and Suzuki, K. 2013. Exercise training attenuates adipose tissue fibrosis in diet-induced obese mice. *Biochem. Biophys. Res. Commun.* **440**: 774–779. [[Medline](#)] [[CrossRef](#)]
22. Khan, T., Muise, E. S., Iyengar, P., Wang, Z. V., Chandalia, M., Abate, N., Zhang, B. B., Bonaldo, P., Chua, S. and Scherer, P. E. 2009. Metabolic dysregulation and adipose tissue fibrosis: role of collagen VI. *Mol. Cell. Biol.* **29**: 1575–1591. [[Medline](#)] [[CrossRef](#)]
23. Kihira, Y., Miyake, M., Hirata, M., Hoshina, Y., Kato, K., Shirakawa, H., Sakaue, H., Yamano, N., Izawa-Ishizawa, Y., Ishizawa, K., Ikeda, Y., Tsuchiya, K., Tamaki, T. and Tomita, S. 2014. Deletion of hypoxia-inducible factor-1 α in adipocytes enhances glucagon-like peptide-1 secretion and reduces adipose tissue inflammation. *PLoS One* **9**: e93856. [[Medline](#)] [[CrossRef](#)]
24. Korsic, M., Gotovac, K., Nikolac, M., Dusek, T., Skegro, M., Muck-Seler, D., Brovecki, F. and Pivac, N. 2012. Gene expression in visceral and subcutaneous adipose tissue in overweight women. *Front. Biosci. (Elite Ed.)* **4**: 2734–2744. [[Medline](#)]
25. Kranendonk, M. E., van Herwaarden, J. A., Stupkova, T., de Jager, W., Vink, A., Moll, F. L., Kalkhoven, E. and Visseren, F. L. J. 2015. Inflammatory characteristics of distinct abdominal adipose tissue depots relate differently to metabolic risk factors for cardiovascular disease: distinct fat depots and vascular risk factors. *Atherosclerosis* **239**: 419–427. [[Medline](#)] [[CrossRef](#)]
26. Kung, C. P. and Murphy, M. E. 2016. The role of the p53 tumor suppressor in metabolism and diabetes. *J. Endocrinol.* **231**: R61–R75. [[Medline](#)] [[CrossRef](#)]
27. Liu, R., Pulliam, D. A., Liu, Y. and Salmon, A. B. 2015. Dynamic differences in oxidative stress and the regulation of metabolism with age in visceral versus subcutaneous adipose. *Redox Biol.* **6**: 401–408. [[Medline](#)] [[CrossRef](#)]
28. Minamino, T., Orimo, M., Shimizu, I., Kunieda, T., Yokoyama, M., Ito, T., Nojima, A., Nabetani, A., Oike, Y., Matsubara, H., Ishikawa, F. and Komuro, I. 2009. A crucial role for adipose tissue p53 in the regulation of insulin resistance. *Nat. Med.* **15**: 1082–1087. [[Medline](#)] [[CrossRef](#)]
29. Mizuno, S., Bogaard, H. J., Kraskauskas, D., Alhussaini, A., Gomez-Arroyo, J., Voelkel, N. F. and Ishizaki, T. 2011. p53 Gene deficiency promotes hypoxia-induced pulmonary hypertension and vascular remodeling in mice. *Am. J. Physiol. Lung Cell. Mol. Physiol.* **300**: L753–L761. [[Medline](#)] [[CrossRef](#)]
30. Motoyama, M., Sasaki, K. and Watanabe, A. 2016. *Wagyu* and the factors contributing to its beef quality: A Japanese industry overview. *Meat Sci.* **120**: 10–18. [[Medline](#)] [[CrossRef](#)]
31. Murano, I., Barbatelli, G., Parisani, V., Latini, C., Muzzonigro, G., Castellucci, M. and Cinti, S. 2008. Dead adipocytes, detected as crown-like structures, are prevalent in visceral fat depots of genetically obese mice. *J. Lipid Res.* **49**: 1562–1568. [[Medline](#)] [[CrossRef](#)]
32. Narita, T., Kobayashi, M., Itakura, K., Itagawa, R., Kabaya, R., Sudo, Y., Okita, N. and Higami, Y. 2018. Differential response to caloric restriction of retroperitoneal, epididymal, and subcutaneous adipose tissue depots in rats. *Exp. Gerontol.* **104**: 127–137. [[Medline](#)] [[CrossRef](#)]
33. Ohfuji, S. 2017. Pathology of muscular steatosis in the bovine species: report of two spontaneously arising cases and comparative overview of the condition. *Comp. Clin. Pathol.* **26**: 237–245. [[CrossRef](#)]
34. Oka, A., Iwamoto, E. and Tatsuda, K. 2015. Effects of clay on fat necrosis and carcass characteristics in Japanese Black steers. *Anim. Sci. J.* **86**: 878–883. [[Medline](#)] [[CrossRef](#)]

35. Olovnikov, A. M. 1996. Telomeres, telomerase, and aging: origin of the theory. *Exp. Gerontol.* **31**: 443–448. [[Medline](#)] [[CrossRef](#)]
36. Poulain-Godefroy, O., Lecoq, C., Pattou, F., Frühbeck, G. and Froguel, P. 2008. Inflammation is associated with a decrease of lipogenic factors in omental fat in women. *Am. J. Physiol. Regul. Integr. Comp. Physiol.* **295**: R1–R7. [[Medline](#)] [[CrossRef](#)]
37. Ravi, R., Mookerjee, B., Bhujwala, Z. M., Sutter, C. H., Artemov, D., Zeng, Q., Dillehay, L. E., Madan, A., Semenza, G. L. and Bedi, A. 2000. Regulation of tumor angiogenesis by p53-induced degradation of hypoxia-inducible factor 1 α . *Genes Dev.* **14**: 34–44. [[Medline](#)]
38. Reggio, S., Pellegrinelli, V., Clement, K. and Tordjman, J. 2013. Fibrosis as a cause or a consequence of white adipose tissue inflammation in obesity. *Curr. Obes. Rep.* **2**: 1–9. [[CrossRef](#)]
39. Robelin, J. 1981. Cellularity of bovine adipose tissues: developmental changes from 15 to 65 percent mature weight. *J. Lipid Res.* **22**: 452–457. [[Medline](#)]
40. Rodier, F. and Campisi, J. 2011. Four faces of cellular senescence. *J. Cell Biol.* **192**: 547–556. [[Medline](#)] [[CrossRef](#)]
41. Salama, R., Sadaie, M., Hoare, M. and Narita, M. 2014. Cellular senescence and its effector programs. *Genes Dev.* **28**: 99–114. [[Medline](#)] [[CrossRef](#)]
42. Schafer, M. J., White, T. A., Evans, G., Tonne, J. M., Verzosa, G. C., Stout, M. B., Mazula, D. L., Palmer, A. K., Baker, D. J., Jensen, M. D., Torbenson, M. S., Miller, J. D., Ikeda, Y., Tchkonja, T., van Deursen, J. M., Kirkland, J. L. and LeBrasseur, N. K. 2016. Exercise prevents diet-induced cellular senescence in adipose tissue. *Diabetes* **65**: 1606–1615. [[Medline](#)] [[CrossRef](#)]
43. Schöttl, T., Kappler, L., Braun, K., Fromme, T. and Klingenspor, M. 2015. Limited mitochondrial capacity of visceral versus subcutaneous white adipocytes in male C57BL/6N mice. *Endocrinology* **156**: 923–933. [[Medline](#)] [[CrossRef](#)]
44. Sermeus, A. and Michiels, C. 2011. Reciprocal influence of the p53 and the hypoxic pathways. *Cell Death Dis.* **2**: e164. [[Medline](#)] [[CrossRef](#)]
45. Shimabukuro, M., Kozuka, C., Taira, S., Yabiku, K., Dagvasumberel, M., Ishida, M., Matsumoto, S., Yagi, S., Fukuda, D., Yamakawa, K., Higa, M., Soeki, T., Yoshida, H., Masuzaki, H. and Sata, M. 2013. Ectopic fat deposition and global cardiometabolic risk: new paradigm in cardiovascular medicine. *J. Med. Invest.* **60**: 1–14. [[Medline](#)] [[CrossRef](#)]
46. Shimizu, I., Yoshida, Y., Katsuno, T., Tateno, K., Okada, S., Moriya, J., Yokoyama, M., Nojima, A., Ito, T., Zechner, R., Komuro, I., Kobayashi, Y. and Minamino, T. 2012. p53-induced adipose tissue inflammation is critically involved in the development of insulin resistance in heart failure. *Cell Metab.* **15**: 51–64. [[Medline](#)] [[CrossRef](#)]
47. Shimizu, I., Yoshida, Y., Suda, M. and Minamino, T. 2014. DNA damage response and metabolic disease. *Cell Metab.* **20**: 967–977. [[Medline](#)] [[CrossRef](#)]
48. Smas, C. M. and Sul, H. S. 1993. Pref-1, a protein containing EGF-like repeats, inhibits adipocyte differentiation. *Cell* **73**: 725–734. [[Medline](#)] [[CrossRef](#)]
49. Tanomura, H., Miyake, T., Taniguchi, Y., Manabe, N., Kose, H., Matsumoto, K., Yamada, T. and Sasaki, Y. 2002. Detection of a quantitative trait locus for intramuscular fat accumulation using the OLETF rat. *J. Vet. Med. Sci.* **64**: 45–50. [[Medline](#)] [[CrossRef](#)]
50. Tchkonja, T., Morbeck, D. E., Von Zglinicki, T., Van Deursen, J., Lustgarten, J., Scoble, H., Khosla, S., Jensen, M. D. and Kirkland, J. L. 2010. Fat tissue, aging, and cellular senescence. *Aging Cell* **9**: 667–684. [[Medline](#)] [[CrossRef](#)]
51. Toussaint, O., Royer, V., Salmon, M. and Remacle, J. 2002. Stress-induced premature senescence and tissue ageing. *Biochem. Pharmacol.* **64**: 1007–1009. [[Medline](#)] [[CrossRef](#)]
52. Umezu, Y., Tanomura, H., Miyake, T., Taniguchi, Y., Manabe, N., Yamada, T. and Sasaki, Y. 2001. Detection of rat model useful for genetic analysis of intramuscular fat accumulation. *J. Anim. Genet.* **29**: 3–10. [[CrossRef](#)]
53. Yahagi, N., Shimano, H., Matsuzaka, T., Sekiya, M., Najima, Y., Okazaki, S., Okazaki, H., Tamura, Y., Iizuka, Y., Inoue, N., Nakagawa, Y., Takeuchi, Y., Ohashi, K., Harada, K., Gotoda, T., Nagai, R., Kadowaki, T., Ishibashi, S., Osuga, J. and Yamada, N. 2004. p53 involvement in the pathogenesis of fatty liver disease. *J. Biol. Chem.* **279**: 20571–20575. [[Medline](#)] [[CrossRef](#)]
54. Yamada, T., Kawakami, S. and Nakanishi, N. 2010. Fat depot-specific differences in angiogenic growth factor gene expression and its relation to adipocyte size in cattle. *J. Vet. Med. Sci.* **72**: 991–997. [[Medline](#)] [[CrossRef](#)]
55. Yamada, T., Higuchi, M. and Nakanishi, N. 2013. Plasma 8-isoprostane concentrations and adipogenic and adipokine gene expression patterns in subcutaneous and mesenteric adipose tissues of fattening Wagyu cattle. *J. Vet. Med. Sci.* **75**: 1021–1027. [[Medline](#)] [[CrossRef](#)]
56. Yamada, T., Higuchi, M. and Nakanishi, N. 2015. Effect of the anatomical site on telomere length and pref-1 gene expression in bovine adipose tissues. *Biochem. Biophys. Res. Commun.* **463**: 923–927. [[Medline](#)] [[CrossRef](#)]
57. Zhao, M. and Chen, X. 2015. Effect of lipopolysaccharides on adipogenic potential and premature senescence of adipocyte progenitors. *Am. J. Physiol. Endocrinol. Metab.* **309**: E334–E344. [[Medline](#)] [[CrossRef](#)]